

Combined heat and power using high-temperature proton exchange membrane fuel cells for housing facilities

Víctor Sanz i López

Institut de Robòtica i Informàtica Industrial (CSIC-UPC)
Barcelona, Catalonia, Spain
vsanz@iri.upc.edu

Guillermo López

Institut de Robòtica i Informàtica Industrial (CSIC-UPC)
Barcelona, Catalonia, Spain
guillermo.lopez@estudiant.upc.edu

Ramon Costa-Castelló

Institut de Robòtica i Informàtica Industrial (CSIC-UPC)
Barcelona, Catalonia, Spain
ramon.costa@upc.edu

Carles Batlle

Institut d'Organització i Control (UPC)
Barcelona, Catalonia, Spain
carles.batlle@upc.edu

Abstract—Recently, new alternatives to conventional energy sources such as fossil fuels are arising due to global problems related to climate change effect and energy shortage. In this context, fuel cells and combined heat and power technologies appear as a possible solution due to their ability to provide both electrical and thermal energy more efficiently compared to traditional methods. Related to this, high-temperature proton exchange membrane fuel cells offer the possibility of implementing combined heat and power systems, and they are also considered an efficient technology that emits less greenhouse gases. In this article a model predictive control based energy management system for a specific house is presented. Simulation and control models of the system are presented, together with dimensions and energy profiles used. Finally, control objectives and the proposed control algorithm are detailed, and the results when trying to match residential heat and power demands are discussed.

Index Terms—energy management, model predictive control, combined heat and power, fuel cells

I. INTRODUCTION

Hydrogen is a very promising energy vector, and fuel cells constitute a technology that allows to obtain electrical energy and heat from it in a very efficient way [1], [2].

In the context of energy efficiency for comfort applications [3], cogeneration or "combined heat and power" (CHP) constitutes a reliable way to take profit of both types of energy, electrical and thermal [4]–[7]. Among different technologies compatible with CHP systems, fuel cells have been used in countries like Japan as an easy way to generate energy locally and close to the consumption point [8], [9]. The fact that thermal energy is released during the energy production process undergoing in fuel cells makes them useful if this energy can be used for thermal purposes like space or water heating, typical of certain industries or housing facilities in general [10]. High-temperature proton exchange membrane fuel cells (HT-PEMFC) operate at temperatures above 100°C and combine hydrogen gas with oxygen to produce water

steam, electrical power and heat [11]–[13]. Although electrical applications of low temperature PEMFC (LT-PEMFC) have been implemented for many years, heat produced by HT-PEMFC can be used and thus increase global efficiency (electrical and thermal) to maximum levels. This is the reason why its use in comfort applications such as housing, where space and water heating are important, is an option being explored in recent years [14]. In this research line, energy management strategies to maximise CHP efficiency are of the utmost importance.

Energy management plays a very important role in CHP, determining the required amount of thermal and electrical energy, and making it compatible with the thermal and electrical demands is not, in general, an easy affair. In the context of process control in general, model predictive control (MPC) is a well known method in many applications like highscale electrical networks or smaller facilities like the one studied in this article [3], [15]. In this context MPC has been studied as a reliable strategy to ensure maximum efficiency at all time of both electrical and thermal consumption [16]–[18]. This control strategy, based on solving a constrained optimisation problem, is able to anticipate the tendency of the system response based on a provided prediction so that control inputs can tend to the possible value needed in following iterations [19], [20]. Therefore, the problem of integrating HT-PEMFC on CHP residential systems and an energy management strategy is one being studied nowadays [21].

In the present article, characterisation and modelling of a HT-PEMFC stack is presented, as well as the auxiliary elements for the CHP system such as heating water deposits and electrical batteries. For doing so, both behavioural characteristics and technical specifications of these systems have been considered. The proposed system model of the CHP system prepared for control is presented. A supervisory control in the shape of a model predictive control in order to

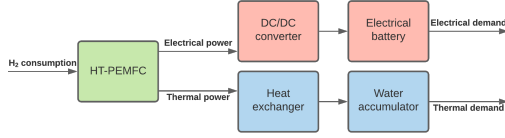


Fig. 1: CHP system elements

manage energy operational constraints is presented after that. Finally, this model predictive control scheme is applied to a prototype house considering different scenarios corresponding to different seasons of the year.

II. SYSTEM MODEL

Fig. 1 shows a scheme of the system architecture under study. As can be seen, the fuel cell is accompanied by a converter and a battery to manage the electrical part of the system, while in the thermal part the presence of a heat exchanger and a thermal storage system is assumed. This architecture is common in this type of system [8]. Storage systems play a decisive role so that the fuel cell can jointly supply thermal and electrical loads.

The role of the different elements in Fig. 1 is the following:

- *HT-PEMFC*: able to generate heat and electrical energy.
- *DC/DC converter*: establishes the desired level of voltage.
- *Battery*: stores electrical energy to be supplied depending on the demand.
- *Heat exchanger*: to connect fuel cell and the water tank when heating it.
- *Water tank*: stores heat for space heating and hot water to be used by humans.

We will use two models to describe the behaviour of this system. First, a detailed model, presented in Section II-A, will be used for the simulation of the system. Subsequently, a simplified linear model will be developed, described in the section II-B, which will be used for the implementation of the control system.

A. Simulation model

Fig. 2 shows the structure of the model used for the simulation. This model has been implemented using MATLAB/Simulink and preserves the structure of the system. This model is the one used for simulation and it includes nonlinearities in fuel cell and electrical battery submodels. Both models used for PEM fuel cell and electrical battery are the ones provided by Matlab/Simulink and they are included with their electrical converters, responsible of regulating connection of different elements to the electrical system, inside blocks seen in Fig. 2. The fuel cell model is described in detail in [22], but it does not take into account heat generated, which has been added in this work. Finally, the water accumulator model has been designed applying a thermal balance between the heat released by the fuel cell, an oil tank being heated by this heat and the water accumulator heated by this oil tank through a heat exchanger. The block tagged as 'Current input'

corresponds to the fuel cell current provided by the energy management strategy detailed later in this article. The ones tagged as 'Thermal input' and 'Electrical input' correspond to additional flows, connections to grid and power transferred between electrical and thermal system. Finally, input blocks tagged as 'Electrical demand' and 'Thermal demand' are treated as disturbances from the point of view of the system. In the case of the thermal input it has two components:

- Heat generated by means of a transfer of electrical to thermal power in case of high thermal demand.
- Heat provided by using water stored in the water accumulator.

Likewise, electrical input has the following three components to be added:

- Electricity transformed to heat and transferred to the thermal part of the CHP system in case of high thermal demand.
- Electrical power supplied by the grid.
- Electrical power supplied to the grid.

Disturbances have the following two components:

- Electrical demand of the housing facility.
- Thermal demand of the housing facility.

In the case of the fuel cell, the curve relating voltage to current is called polarisation curve and, in the model used it is the one seen in Fig. 3. In the case studied, a stack of 72 fuel cells designed for temperatures above water's boiling point is used. The thermal and electrical power provided by the fuel cell can be seen in Fig. 4.

B. Control model

Although it is possible to propose an MPC controller for a non-linear and complex model like the one proposed in the previous section, in order to obtain an easily implementable controller, a linear model will be created that keeps the main characteristics of the initial model. This model will be directly formulated as a discrete-time state-space model.

The state vector is defined as

$$\mathbf{x} = \begin{bmatrix} E_{elec}^{bat} \\ E_{therm}^{acc} \end{bmatrix} \quad (1)$$

formed by the following 2 states:

- Stored electrical energy in the battery E_{elec}^{bat} .
- Stored thermal energy in the water accumulator E_{therm}^{acc} .

Additionally, the system has a total of 5 inputs in input vector \mathbf{u} and 2 variables in disturbance vector \mathbf{d} :

$$\mathbf{u} = \begin{bmatrix} I_{fc} \\ W_{tra} \\ W_{grid_{in}} \\ W_{grid_{out}} \\ W_{accum_{out}} \end{bmatrix}, \quad \mathbf{d} = \begin{bmatrix} W_{d_{elec}} \\ W_{d_{therm}} \end{bmatrix} \quad (2)$$

These variables stand for:

- Fuel cell current I_{fc} .
- Electrical to thermal transfer resistance W_{tra} .

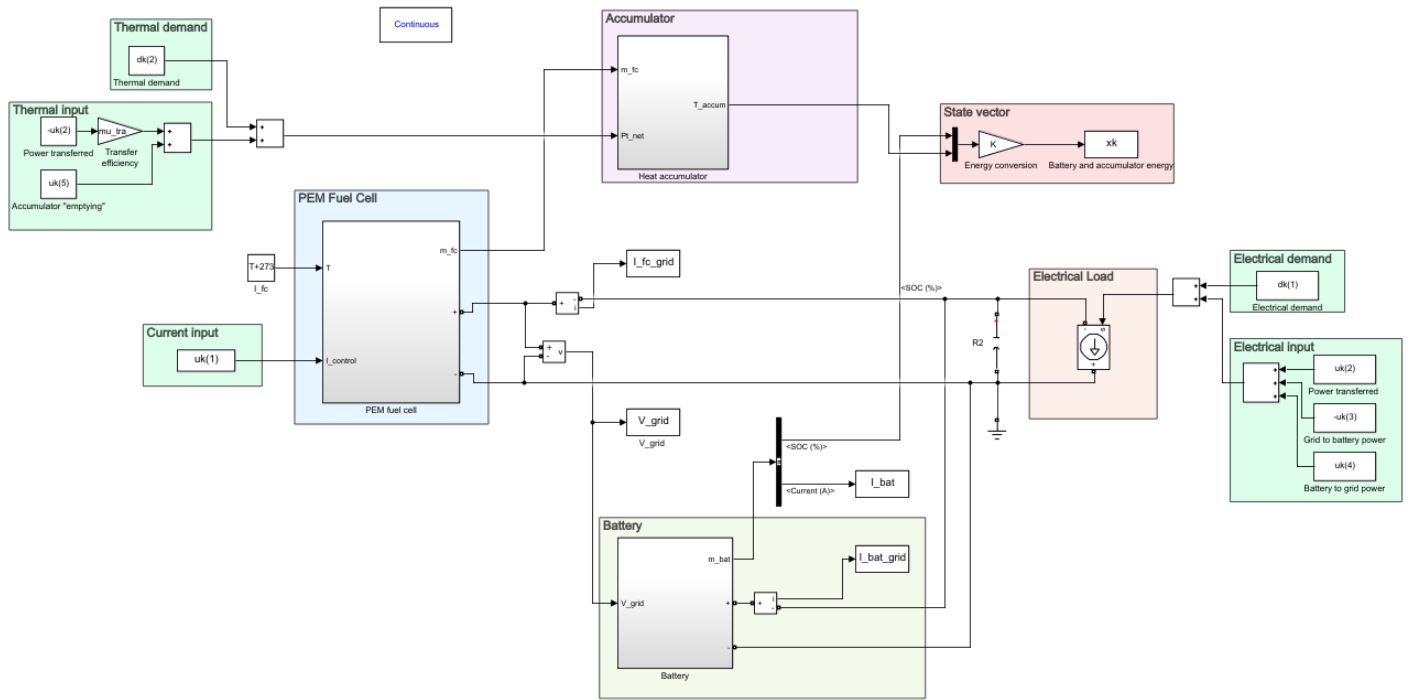


Fig. 2: Nonlinear system model in Simulink

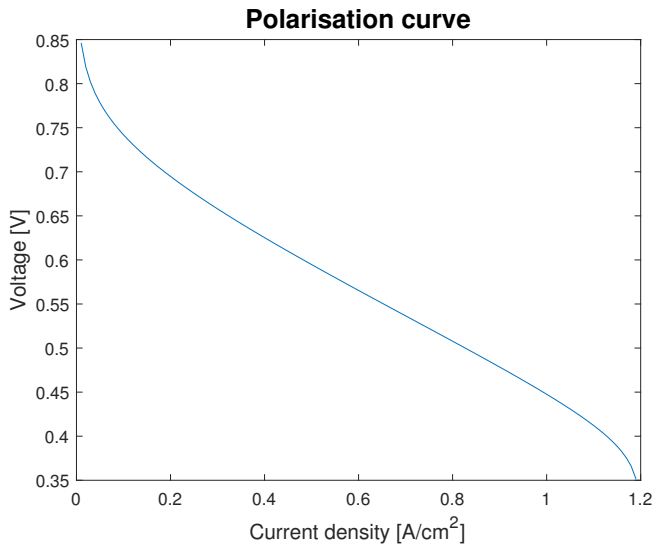


Fig. 3: Polarisation curve of the studied fuel cell

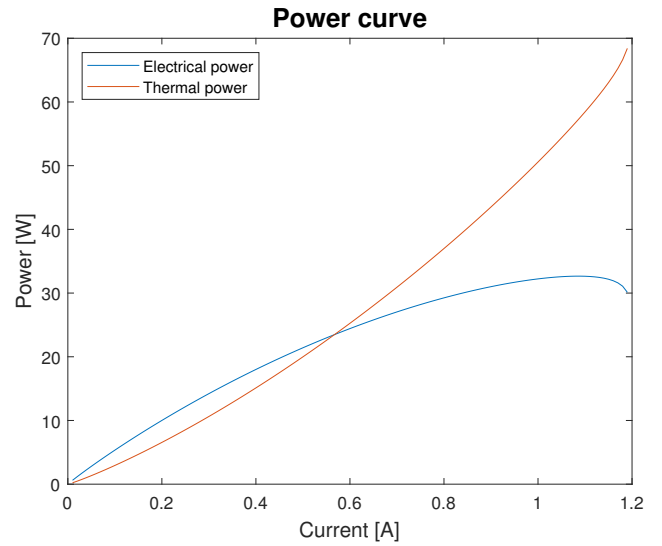


Fig. 4: Thermal and electrical power provided by the whole fuel cell stack

- 3 security elements to connect to grid and the accumulator if necessary for demand purposes $W_{grid_{in}}$, $W_{grid_{out}}$ and $W_{accum_{out}}$.
- Electrical and thermal demands $W_{d_{elec}}$ and $W_{d_{therm}}$ are considered as disturbances.

The model can be written as:

$$\begin{aligned} \mathbf{x}_{k+1} &= \mathbf{A}\mathbf{x}_k + \mathbf{B}\mathbf{u}_k + \mathbf{G}_d\mathbf{d}_k \\ \mathbf{y}_k &= \mathbf{C}\mathbf{x}_k \end{aligned} \quad (3)$$

where

$$\begin{aligned} \mathbf{A} &= \begin{bmatrix} 1 & 0 \\ 0 & 1 - \frac{K_{conv}T_s}{m_{acc}C_{H_2O}} \end{bmatrix}, \\ \mathbf{B} &= T_s \begin{bmatrix} \eta_{conv}V_{fc}^{nom} & \eta_{exch}(V_q^{nom} - V_{fc}^{nom}) \\ -1 & \eta_{tra} \\ 1 & 0 \\ -1 & 0 \\ 0 & -1 \\ -1 & 0 \\ 0 & -1 \end{bmatrix}^T, \\ \mathbf{C} &= \mathbf{I}_{2 \times 2}, \quad \mathbf{G}_d = -T_s. \end{aligned} \quad (4)$$

The parameters used in the model are:

- K_{env} , environment losses constant.
- T_s , sampling time of the model predictive control.
- m_{acc} , mass of water in the accumulator.
- C_{H_2O} , water's specific heat.
- η_{conv} , converter efficiency.
- η_{exch} , heat exchanger efficiency.
- η_{tra} , transfer resistance.
- V_{fc}^{nom} , electrical voltage due to linearisation.
- V_q^{nom} , thermal voltage due to linearisation.

Using this linearised model a model predictive control is designed as explained in Section IV and compared with the non-linear simulation model.

III. CONTROL OBJECTIVES

When designing the CHP system, the main target is being able to feed both the thermal and the electrical demand in an efficient manner. In order to apply an MPC controller, it is necessary to transform this generic objective into a cost function and restrictions on the system variables. As usual in the MPC [19], [23], in this work the cost function will be constructed as the linear combination of different cost functions, each of which will be directly related to a specific concept. All norms used represent 1-norm. This will lead to what is known as a multi-objective optimization problem. This optimisation problem is solved for every iteration, separated by a sample time, and the following ones are predicted. For this, $u_{k,i}$ is defined as the i -component of the input vector (equation (2)) for a certain iteration k .

The objective functions that will be considered in this work are

- Consumed hydrogen: Consumed hydrogen is proportional to the fuel cell current [11]. Consequently, the following cost function is proposed:

$$f_{i,1} = \frac{\|u_{k+i,1}\|_1}{I_{fc,max}} \quad (5)$$

- Fuel cell current variation: fast variation in the fuel cell current might produce starvation in the fuel cell which is one of the main degradation sources [11]. To minimize this, the following cost function is suggested:

$$f_{i,2} = \frac{\|u_{k+i,1} - u_{k+i-1,1}\|_1}{I_{fc,max}} \quad (6)$$

- Minimising energy: e_k a variable (equation (8)) to change power flow between battery and the grid, so that energy used can adapt to demand. To minimise energy consumption using methods like the external grid, the following cost function is defined:

$$f_{i,3} = \|e_{k+i}\|_1 \quad (7)$$

$$e_k = \{0, 1\} \quad (8)$$

- Minimising electrical power transferred to the thermal system. In case extra thermal demand is needed, thermal

energy can be produced due to Joule's effect with an appropriate electrical space heating device:

$$f_{i,4} = \frac{\|u_{k+i,2}\|_1}{P_{tra}^{max}} \quad (9)$$

- Minimising variation of electrical power transferred to the thermal system, using values from two consecutive iterations ($k-1$ and k). The reason is that this transfer should be smooth enough in time and activate just when needed for long time intervals, not just concrete instants:

$$f_{i,5} = \frac{\|u_{k+i,2} - u_{k-1,2}\|_1}{P_{tra}^{max}} \quad (10)$$

- Minimising electrical power supplied by the grid, when the system is not able to supply enough energy or when extra energy demand would require the system to violate constraints or neglect other control objectives:

$$f_{i,6} = \frac{\|u_{k+i,4}\|_1}{P_{e,loss}^{max}} \quad (11)$$

- Minimising variation of electrical power supplied by the grid, using values from two consecutive iterations ($k-1$ and k) to prevent sudden variations that may damage systems like the electrical battery [24]:

$$f_{i,7} = \frac{\|u_{k+i,4} - u_{k+i-1,4}\|_1}{P_{e,loss}^{max}} \quad (12)$$

- Minimising electrical power supplied to the grid, to ensure that extra energy is not produced all the time by the system. Just when extra electrical energy is produced, when thermal demand is much higher than the electrical one, electrical energy not needed is supplied to the grid:

$$f_{i,8} = \frac{\|u_{k+i,3}\|_1}{P_{e,loss}^{max}} \quad (13)$$

- Minimising variation of electrical power supplied to the grid, using values from two consecutive iterations ($k-1$ and k), to ensure extra energy is only discarded when it is too high during a certain amount of time:

$$f_{i,9} = \frac{\|u_{k+i,3} - u_{k+i-1,3}\|_1}{P_{e,loss}^{max}} \quad (14)$$

- Minimising thermal power extracted as waste, as only extra heat must be discarded for safety reasons related with environment heating:

$$f_{i,10} = \frac{\|u_{k+i,5}\|_1}{P_{t,loss}^{max}} \quad (15)$$

- Minimising variation of thermal power extracted as waste, using values from two consecutive iterations ($k-1$ and k). This is only done in cases when heat is discarded in long intervals, not just specific instants:

$$f_{i,11} = \frac{\|u_{k+i,5} - u_{k+i-1,5}\|_1}{P_{t,loss}^{max}} \quad (16)$$

IV. MODEL PREDICTIVE CONTROL FORMULATION

To match the values of heat and electrical power generated to the demand in the case of a specific house a model predictive control problem is formulated. The system state space obtained from a thermal and electrical balance is used as a constraint for the optimisation problem in its discretised form. The objective function is calculated adding up all control objectives presented in the previous section $f_{i,j}$, each of them with its weight function w_j , to prioritise some objectives above others.

System model constraints are the ones from the state-space model previously presented in equations (3) and (4), considering demands as disturbance \mathbf{d}_k and including them as inputs. This model's variables are constrained with upper and lower bounds, using soft constraints, which should be avoided when possible, and hard constraints, which cannot be violated. All these constraints are included in constraints vector $\mathbf{g} = [g_1, \dots, g_{24}]$, with each inequality with index j corresponding to a component g_j of vector \mathbf{g} . These constraints are applied to different variables and are organised and described as follows:

Current constraints g_1 to g_4 limiting its boundary values and variation in consecutive instants are:

$$\begin{aligned} I_{fc,min} &\leq u_{k,1} \leq I_{fc,max} \\ -dI_{fc,max} &\leq u_{k,1} - u_{k-1,1} \leq dI_{fc,max} \end{aligned} \quad (17)$$

Electrical energy constraints g_5 and g_6 limiting its boundary values (using binary variable e_k limited by g_9 and g_{10} to enable soft constraints) and thermal energy boundaries g_7 and g_8 are:

$$\begin{aligned} x_{k+1} &\geq E_{e,llim} - (E_{e,llim} - E_{e,min})e_k \\ x_{k+1} &\leq E_{e,hlim} + (E_{e,max} - E_{e,llim})e_k \\ E_{t,min} &\leq x_{k+1,2} \leq E_{t,max} \\ 0 &\leq e_k \leq 1 \end{aligned} \quad (18)$$

Electrical power transferred to heat constraints g_{11} to g_{12} , limiting its boundary values and variation in consecutive instants are:

$$P_{tra,min} \leq u_{k,2} \leq P_{tra,max} \quad (19)$$

Electrical battery soft constraints g_{13} and g_{14} (using binary variable y_k to define them) and battery's electrical losses boundaries g_{15} and g_{16} are:

$$\begin{aligned} y_k &\leq (Batt_{ll} - x_{k+1,1})E_{e,max} + 1 \\ u_{k,3} &\leq P_{e,loss}^{max} y_k \\ P_{e,loss}^{min} &\leq u_{k,3} \leq P_{e,loss}^{max} \end{aligned} \quad (20)$$

Battery to grid soft constrains g_{17} to g_{18} (using binary variable y_k to define them) and boundaries of the electrical power exchanged between the battery and the grid g_{19} and g_{20} are:

$$\begin{aligned} y_k &\leq \frac{x_{k+1,1} - Batt_{hl}}{E_{e,max}} + 1 \\ u_{k,4} &\leq P_{e,loss}^{max} y_k \\ P_{e,loss}^{min} &\leq u_{k,4} \leq P_{e,loss}^{max} \end{aligned} \quad (21)$$

Accumulator emptying constraints g_{21} and g_{22} (using binary variable y_k to define them) and thermal power boundaries g_{23} and g_{24} are:

$$\begin{aligned} y_k &\leq \frac{x_{k+1,2} - Accu_{hl}}{E_{t,max}} + 1 \\ u_{k,5} &\leq P_{t,loss}^{max} y_k \\ P_{t,loss}^{min} &\leq u_{k,5} \leq P_{t,loss}^{max} \end{aligned} \quad (22)$$

with variables standing for:

- \mathbf{x}_k is the state vector defined in equation (1). Its first component $x_{k,1}$ corresponds to the electrical energy in the battery E_{elec}^{bat} and the second one, $x_{k,2}$, corresponds to the thermal energy in the water accumulator E_{therm}^{acc} .
- \mathbf{u}_k is the input vector defined in equation (2) with variables defined in the discrete domain. Its first component $u_{k,1}$ corresponds to the HT-PEMFC inlet electrical current I_k , proportional to hydrogen flow. Elements $u_{k,2}$ to $u_{k,5}$ are variables W_{tra} , $W_{grid,in}$, $W_{grid,out}$, $W_{accum,out}$ also defined in equation (2).
- $\mathbf{d}_k = [D_{elec}, D_{therm}^{HW} + D_{therm}^{SH}]^T$ is the disturbance vector composed by expected electricity demand D_{elec} and thermal energy for hot water D_{therm}^{HW} and space heating D_{therm}^{SH} . It corresponds to the last 2 values of \mathbf{u}_k , i.e. $u_{k,6}$ and $u_{k,7}$.
- e_k is a binary variable so that when $e_k = 0$, only soft constraint values remain, forcing the state of charge to be between both. On the contrary, when $e_k = 1$, the soft constraints term cancels out and the battery state of charge is limited between its minimum and maximum values
- y_k is a binary variable that, when set as 0, prevents the input from activating (equation (20)). The first inequality in equation (21) is the responsible of forcing the binary variable to 0 when the state of charge is above a set value.
- $Batt_{min}$, $Batt_{l1}$, $Batt_{h1}$, $Batt_{max}$ are minimum, lowest recommended, highest recommended and maximum battery limits.
- $Accu_{min}$, $Accu_{h1}$, $Accu_{max}$ are minimum, highest recommended and maximum accumulator temperatures.
- $I_{fc,min}$, $I_{fc,max}$ are minimum and maximum electrical current limits.
- $dI_{fc,min}$, $dI_{fc,max}$ are minimum and maximum electrical current variation limits.
- P_{tra}^{min} , P_{tra}^{max} are minimum and maximum transfer resistance limits.
- $P_{e,loss}^{min}$, $P_{e,loss}^{max}$ are minimum and maximum electrical valve limits.
- $P_{t,loss}^{min}$, $P_{t,loss}^{max}$ are minimum and maximum thermal valve limits.

All these constraints g_j are included in a vector $\mathbf{g} = [g_1, \dots, g_{24}]$ and the global cost function, formed adding up all control objectives from equations (5) to (16), is defined as follows:

$$J(\mathbf{x}_k, \mathbf{u}_k) = \sum_{i=0}^{N_{total}} \sum_{j=1}^{11} w_j \cdot f_{i,j}(\mathbf{x}_k, \mathbf{u}_k) \quad (23)$$

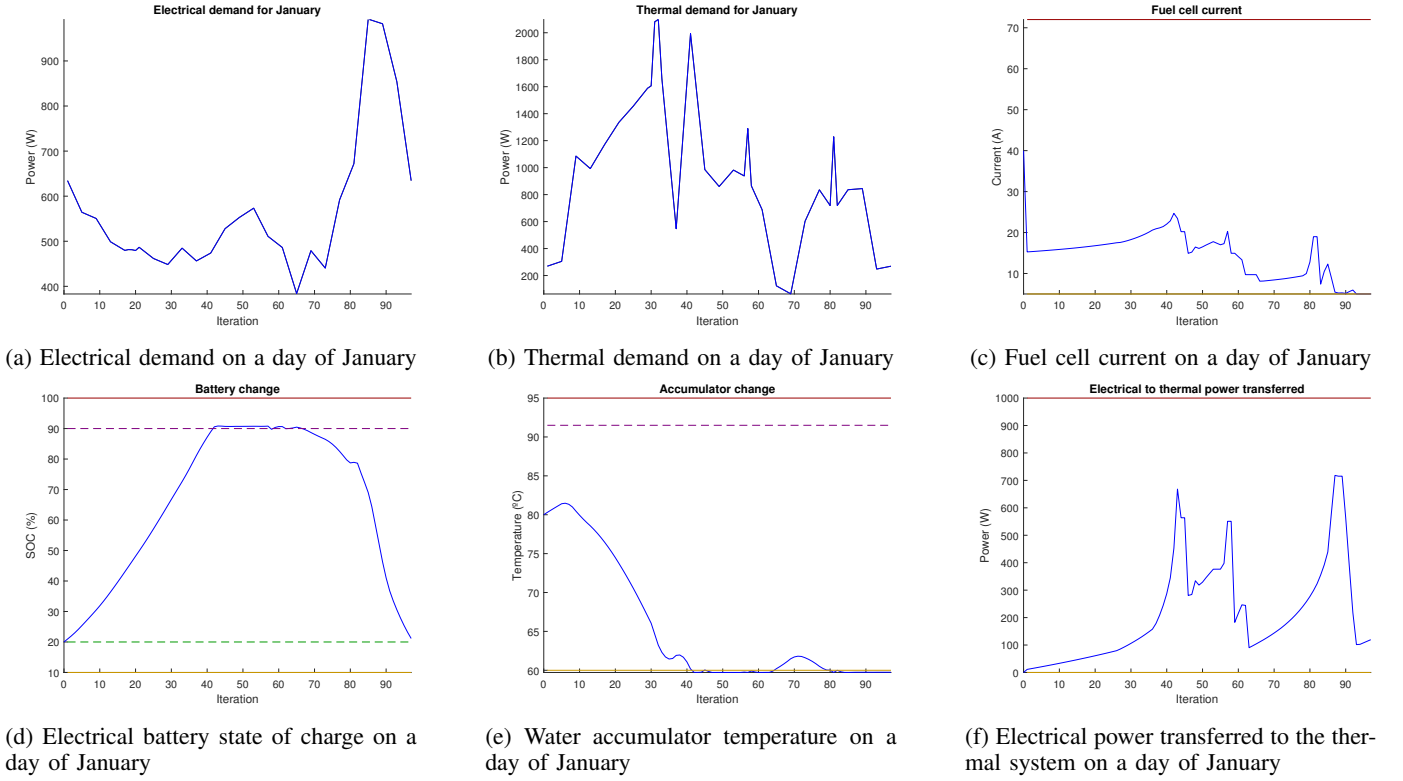


Fig. 5: Results for a day of January

Using this cost function, the optimisation problem is defined as follows:

$$\begin{aligned} \min_{\mathbf{u}_k} J(\mathbf{x}_k, \mathbf{u}_k) \\ \text{subject to} \quad \text{equations (3), (4) and } \mathbf{g} \end{aligned} \quad (24)$$

The steps to be followed during the control process are:

- A prediction horizon for the problem N_{total} and a control horizon $N < N_{total}$ are defined.
- Expected demand values for horizon N are defined, $\hat{\mathbf{d}}_k \cdots \hat{\mathbf{d}}_{k+N}$.
- The optimisation problem to obtain the control action u_k is solved so that the following N predicted states $\hat{\mathbf{x}}_k \cdots \hat{\mathbf{x}}_{k+N}$ match the specifications.
- The process is repeated for each instant k .

Using values presented before, an optimisation problem as shown in equation (24) is implemented. Prediction horizon is selected based on the problem studied, so a whole day is predicted in advance, knowing the energy demand from other years in the same system and day of the month. This means that demand, considered as disturbance, is known, as it does not vary that much from one year to another. This simplifies the problem, as the iterations predicted are close enough to results obtained when time reaches instants previously predicted. To compute the problem with constraints, Yalmip environment is embedded in Matlab. Yalmip is a toolbox able to implement linear matrix inequalities in optimisation problems, as the case of MPC constraints.

V. SIMULATION RESULTS

The control algorithm from previous section is tested in the house model detailed above, in different scenarios. These correspond to a whole day with electrical and thermal demands associated to different months of the year. The time between iterations k used for the prediction is 15 minutes and the prediction horizon is $N_{total} = 97$ (a full day). Weight functions used are selected so that the most important control objectives are prioritised. Those are the ones aimed at minimising hydrogen consumption, extra thermal energy obtained from the electrical system, electrical energy interchanged with the grid and thermal energy released to the environment. Objectives related to smoothness of results are imposed using low weight functions. To obtain the specific weight function values, several simulations are done to select them (TABLE I):

For each scenario, the following variables are monitored:

- Electrical demand.
- Thermal demand.
- Fuel cell current or intensity
- Battery state of charge in percentage.
- Water accumulator temperature.
- Electrical power transferred to add additional heat through a resistance.
- Electrical battery power input, coming from the grid.
- Electrical battery power output, going to the grid.

To test whether the control strategy works as expected

Weight functions w_j	
w_1	0.078
w_2	0.005
w_3	0.005
w_4	0.156
w_5	0.005
w_6	0.195
w_7	0.005
w_8	0.195
w_9	0.005
w_{10}	0.195
w_{11}	0.005

TABLE I: Selected weight functions used for simulation

battery state of charge and water accumulator temperature cannot exceed their minimum and maximum values, imposed by the previously mentioned constraints. Fuel cell current should also stay between certain limits. Additionally, some scenarios may need extra heat, in case of too high thermal demand, or extra heat may be extracted as waste, when thermal demand is too low. Both phenomena will be included in extra plots when they are not zero, and a similar thing is done for electrical power going in or out of the external electrical grid.

Demand profiles are defined according to those of a house located by the sea in the Spanish Mediterranean coast, not considering Summer season, as it is not demanding enough in terms of thermal demand. Results for a typical day of January are the ones seen in Fig. 5. Top and bottom hard constraints are indicated by solid lines and soft constraints by dotted lines.

It can be seen that fuel cell current is low enough and does not present sudden changes (Fig. 5c), the state of charge of the electrical battery remains between boundaries (Fig. 5d) and water in the accumulator keeps a reasonable temperature (Fig. 5e). Additionally, extra thermal power is obtained from the electrical system to match the high thermal demand (Fig. 5f). A similar study is done for April and the corresponding results are displayed in Fig. 6.

The main difference with the case of January is that extra heat produced is not used as thermal demands are not that high (Fig. 6f). This lower thermal demand is responsible for having a higher water temperature in the accumulator (Fig. 6e), which is close to the upper constraint limit. This is the opposite behaviour to the January scenario, where this temperature was close to the lower constraint limit, due to constant use of water for thermal purposes.

Summarising, the algorithm proposed is able to ensure efficiency in hydrogen consumption, using electrical energy from the battery without discharging it below soft constraints and doing the same with thermal energy stored heating water in the accumulator. Temperature of the accumulator reaches high and low constraints, but these events are not permanent and are corrected in following iterations. Thermal power is released to the environment when extra heat is produced and, on the contrary, extra heat is produced using extra electrical power in cases when cold weather requires higher thermal demand. This is deeply influenced by the dimensions of the fuel cell, battery and water accumulator, knowing that

the bigger these elements are, the better the system works. However, extra cost is avoided using smaller devices.

VI. CONCLUSION

An energy management strategy for residential applications based on high-temperature PEM fuel cells has been presented. A mathematical model of the whole combined heat and power system has been described and a version of it has been integrated in a model predictive control problem aimed to maximise efficiency, minimise fuel cell hydrogen consumption and managing electrical battery, water accumulator and other intermediate systems to ensure that comfort demands are met. A multi-objective cost function has been defined, and the intended effect of the individual terms has been discussed. Finally, this control strategy has been tested in simulation using the nonlinear model designed with Matlab/Simulink in two scenarios, corresponding to winter and beginning of spring, as examples of situations with different thermal demands.

Results obtained show that the system is able to adapt to scenarios when thermal demand is high or low, activating additional connections between the electrical and thermal parts of the CHP system included for the sake of safety in real life applications. As future work, a more detailed CHP system where elements are better characterised is possible, so that results are closer to reality. More specifically, if the equivalent linearised model used as constraint of the MPC were closer to the nonlinear system its ability to predict and react to highly variable demands would presumably improve. A formal procedure using Pareto fronts would also improve selection of weight functions more appropriately in future versions of this work.

ACKNOWLEDGMENT

This work has been partially funded by the Spanish national project DOVELAR (ref. RTI2018-096001-B-C32). This work is partially funded by AGAUR of Generalitat de Catalunya through the Advanced Control Systems (SAC) group grant (2017 SGR 482).

REFERENCES

- [1] A. Cecilia, M. Serra, and R. Costa-Castelló, "Nonlinear adaptive observation of the liquid water saturation in polymer electrolyte membrane fuel cells," *Journal of Power Sources*, vol. 492, p. 229641, 2021.
- [2] J. Luna, R. Costa-Castelló, and S. Strahl, "Chattering free sliding mode observer estimation of liquid water fraction in proton exchange membrane fuel cells," *Journal of the Franklin Institute*, vol. 357, no. 18, pp. 13 816 – 13 833, 2020.
- [3] T. Péan, J. Salom, and R. Costa-Castelló, "Price and carbon-based energy flexibility of residential heating and cooling loads using model predictive control," *Sustainable Cities and Society*, p. 101579, 2019.
- [4] H. R. Ellamla, I. Staffell, P. Bujlo, B. G. Pollet, and S. Pasupathi, "Current status of fuel cell based combined heat and power systems for residential sector," *Journal of Power Sources*, vol. 293, pp. 312–328, 2015.
- [5] J. Renau, V. García, L. Domenech, P. Verdejo, A. Real, A. Giménez, F. Sánchez, A. Lozano, and F. Barreras, "Novel use of green hydrogen fuel cell-based combined heat and power systems to reduce primary energy intake and greenhouse emissions in the building sector," *Sustainability*, vol. 13, no. 4, 2021.
- [6] H. O. Alwan, H. Sadeghian, and S. Abdelwahed, "Energy management optimization and voltage evaluation for residential and commercial areas," *Energies*, vol. 12, no. 9, 2019.

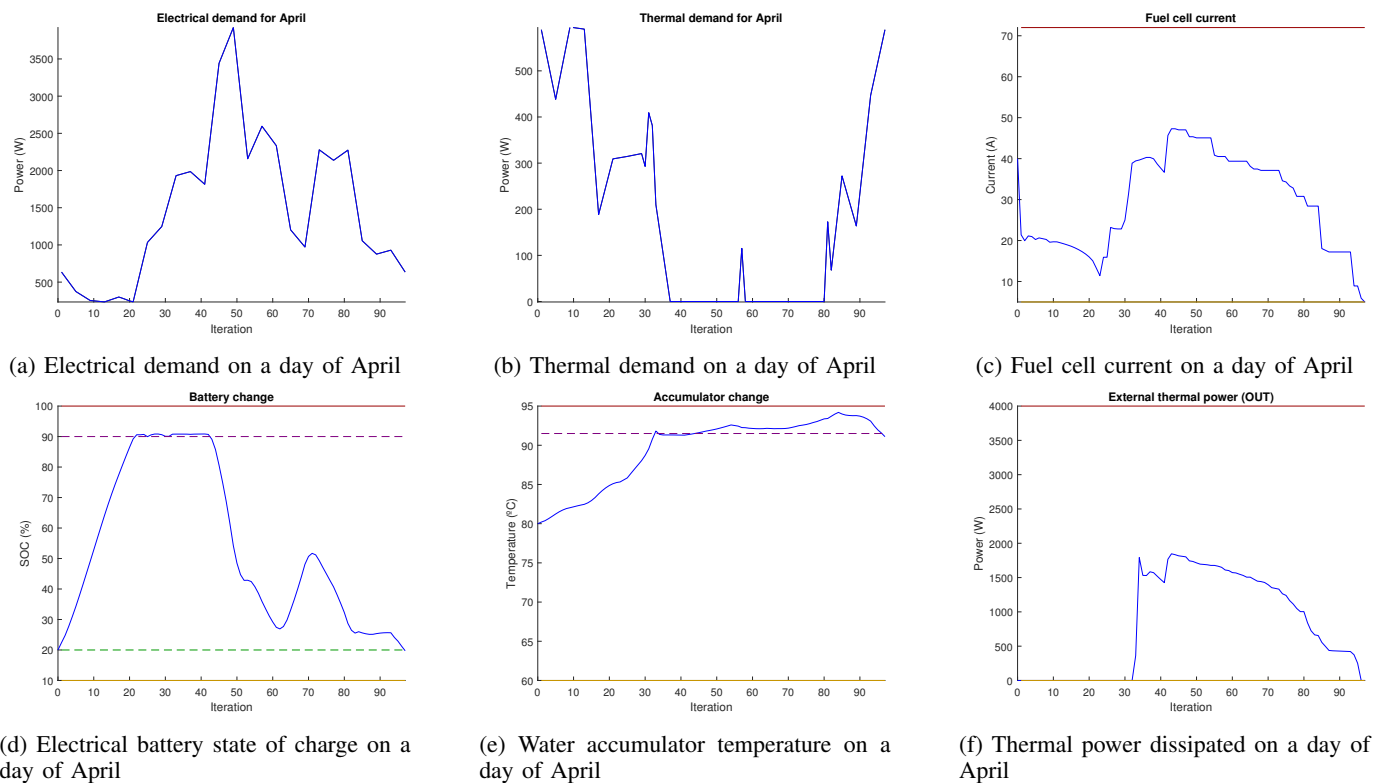


Fig. 6: Results for a day of April

- [7] L. Merkert, A. A. Haime, and S. Hohmann, "Optimal scheduling of combined heat and power generation units using the thermal inertia of the connected district heating grid as energy storage," *Energies*, vol. 12, no. 2, 2019.
- [8] P. Martínez, M. Serra, and R. Costa-Castelló, "Modeling and control of htpemfc based combined heat and power for confort control," in *2017 22nd IEEE International Conference on Emerging Technologies and Factory Automation (ETFA)*, pp. 1–6, Sep. 2017.
- [9] N. Sarabchi, M. Yari, and S. S. Mahmoudi, "Exergy and exergoeconomic analyses of novel high-temperature proton exchange membrane fuel cell based combined cogeneration cycles, including methanol steam reformer integrated with catalytic combustor or parabolic through solar collector," *Journal of Power Sources*, vol. 485, p. 229277, 2021.
- [10] S. N. Giménez, J. M. H. Durá, F. X. B. Ferragud, and R. S. Fernández, "Design and experimental validation of the temperature control of a pemfc stack by applying multiobjective optimization," *IEEE Access*, vol. 8, pp. 183 324–183 343, 2020.
- [11] D. Hissel and M. Pera, "Diagnostic & health management of fuel cell systems: Issues and solutions," *Annual Reviews in Control*, vol. 42, pp. 201–211, 2016.
- [12] R. Rosli, A. Sulong, W. Daud, M. Zulkifley, T. Husaini, M. Rosli, E. Majlan, and M. Haque, "A review of high-temperature proton exchange membrane fuel cell (ht-pemfc) system," *International Journal of Hydrogen Energy*, vol. 42, no. 14, pp. 9293–9314, 2017, special Issue on Sustainable Fuel Cell and Hydrogen Technologies: The 5th International Conference on Fuel Cell and Hydrogen Technology (ICFCHT 2015), 1-3 September 2015, Kuala Lumpur, Malaysia.
- [13] S. S. Araya, F. Zhou, V. Liso, S. L. Sahlin, J. R. Vang, S. Thomas, X. Gao, C. Jeppesen, and S. K. Kr, "A comprehensive review of pbi-based high temperature pem fuel cells," *International Journal of Hydrogen Energy*, vol. 41, no. 46, pp. 21 310–21 344, 2016.
- [14] S. Foresti, G. Manzolini, and S. Escibano, "Experimental investigation of pem fuel cells for a m-chp system with membrane reformer," *International Journal of Hydrogen Energy*, vol. 42, no. 40, pp. 25 334–25 350, 2017.
- [15] J. Köhler, M. A. Müller, and F. Allgöwer, "Distributed model predictive controlrecursive feasibility under inexact dual optimization," *Automatica*, vol. 102, pp. 1–9, 2019.
- [16] Y. Löhr, D. Wolf, C. Pollerberg, A. Hörsting, and M. Mönnigmann, "Supervisory model predictive control for combined electrical and thermal supply with multiple sources and storages," *Applied Energy*, vol. 290, p. 116742, 2021.
- [17] H. He, S. Quan, F. Sun, and Y.-X. Wang, "Model predictive control with lifetime constraints based energy management strategy for proton exchange membrane fuel cell hybrid power systems," *IEEE Transactions on Industrial Electronics*, vol. 67, no. 10, pp. 9012–9023, 2020.
- [18] S. Kuboth, F. Heberle, A. König-Haagen, and D. Brüggemann, "Economic model predictive control of combined thermal and electric residential building energy systems," *Applied Energy*, vol. 240, pp. 372–385, 2019.
- [19] A. Cecilia, J. Carroquino, V. Roda, R. Costa-Castelló, and F. Barreras, "Optimal energy management in a standalone microgrid, with photovoltaic generation, short-term storage, and hydrogen production," *Energies*, vol. 13, no. 6, p. 1454, Mar. 2020.
- [20] U. R. Nair and R. Costa-Castelló, "A model predictive control-based energy management scheme for hybrid storage system in islanded microgrids," *IEEE Access*, vol. 8, pp. 97 809–97 822, 2020.
- [21] T. Kneiske, F. Niedermeyer, and C. Boelling, "Testing a model predictive control algorithm for a pv-chp hybrid system on a laboratory test-bench," *Applied Energy*, vol. 242, pp. 121–137, 2019.
- [22] S. N. Motapon, O. Tremblay, and L. A. Dessaint, "Development of a generic fuel cell model: Application to a fuel cell vehicle simulation," *International Journal of Power Electronics*, vol. 4, no. 6, pp. 505–522, 2012.
- [23] U. R. Nair, M. Sandelic, A. Sangwongwanich, T. Dragicevic, R. Costa-Castelló, and F. Blaabjerg, "An analysis of multi objective energy scheduling in pv-bess system under prediction uncertainty," *IEEE Transactions on Energy Conversion*, pp. 1–11, 2021.
- [24] X. Hu, C. Martinez, and Y. Yang, "Charging, power management, and battery degradation mitigation in plug-in hybrid electric vehicles: A unified cost-optimal approach," *Mechanical Systems and Signal Processing*, vol. 87, pp. 4–16, 2017.